A Multi-Feature Visibility Processing Algorithm for Radio Interferometric Imaging

Mu-Min Chiou[1], Jean-Fu Kiang[1], and Raj Mittra[2]
[1]Graduate Institute of Communication Engineering, National Taiwan University, Taipei, Taiwan 106, ROC
[2]EMC Laboratory, the Pennsylvania State University, University Park, PA 16802, USA

***Abstract* - A computationally efficient multi-feature image reconstruction algorithm, well adapted for next-generation telescopes, is proposed. This method is more flexible to handle vast amount of visibility data expected in the future. In reconstructing the M87 image with the visibility data simulated on the Low-Frequency Array (LOFAR), this algorithm turns out to be a few hundreds to one thousand times faster and is more resilient to noises than the conventional algorithms.**

***Index Terms* — Radio interferometry, image reconstruction, visibility, LOFAR.**

I. INTRODUCTION

Radio interferometry techniques have been used to reconstruct images of astrophysical objects using incomplete and noisy visibility data. By augmenting more stations into an existing telescope, higher angular resolution and sensitivity can be achieved [1]. In general, the image reconstruction process with radio interferometry can be formulated as a linear inverse problem, in which the available measurement data are used to reconstruct the source image, subject to certain constraints [2].

Next-generation radio telescopes, such as Square Kilometre Array Pathfinder (ASKAP) [3], Murchinson Widefield Array (MWA) [4], Meerkat [5], Square Kilometre Array (SKA) [6], and Low-Frequency Array (LOFAR) [7], are expected to achieve a wider dynamic range and higher angular resolution than current instruments. These telescopes will record vast amount of data.

In this work, a multi-feature algorithm is proposed to process four different features of the visibility data separately, with the data simulated on the LOFAR configuration. This method is driven by the measurement data, without the need of a prior function for regularization. It takes much shorter computational time and is more resilient to noises than the conventional methods.

II. MULTI-FEATURE VISIBILITY DISTRIBUTION

Fig.1(a) shows the image intensity of M87 with 256x256 pixels, which is located at the declination of 12°23'28". The image is taken at 140 MHz, with resolutions of $\triangle\theta_u$=3.4" and $\triangle\theta_v$= 3.1".

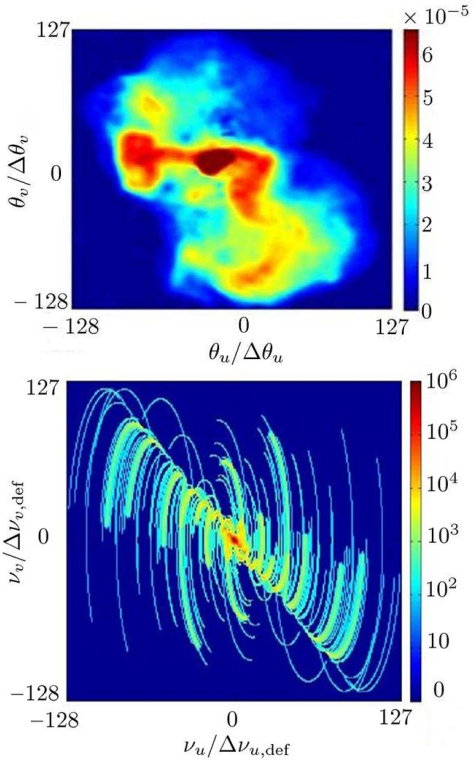

Fig. 1. (a) LOFAR image of M87 near the center of Virgo cluster. (b) Number density of visibility data in the visibility plane.

Fig.1(b) displays the number density of simulated visibility data when observing the M87. The sampling interval is 60 seconds, and the total observation time is 6 hours. The visibility data collected from the CS-CS (core station) links concentrate around the origin, which bear low-resolution information of the image. The visibility data collected from the CS-RS (remote station) links usually take the shape of ribbons; and those from the RS-RS links take the string shape, both bear high-resolution information.

III. MULTI-FEATURE ALGORITHM

The multi-feature algorithm processes the four different types of feature separately. It can be scaled up to include additional stations, such as the international stations in the LOFAR. The multi-feature algorithm can also be adapted for parallel computation, which is more flexible to deal with the

vast amount of data the next-generation telescopes will collect.

In each visibility region, a grid with an optimized cell size is chosen to derive a set of modeled visibility data, using the Broyden-Fletcher-Goldfarb-Shanno (BFGS) algorithm [8], which is a variant of the quasi-Newton's method.

The quality of reconstruction can be evaluated in terms of a signal-to-noise ratio (SNR), where the noise term is defined as the difference between the reconstructed image and the reference image. A higher SNR value implies better quality of the reconstructed image.

Similar to SNR, an ISNR is defined, with the image data replaced by the visibility data. Fig.2 shows the average SNR of the reconstructed image, as a function of ISNR, over 100 realizations of Monte-Carlo simulation.

If 6 hours of measurement is considered, at the sampling interval of 60 seconds, there will be 504,720 visibility data points. The SNR values of the images reconstructed with the multi-feature algorithm and the conventional MS-CLEAN algorithm are 23.414 dB and 19.417 dB, respectively.

If the data sampling interval is reduced to 2 seconds, there will be 15,141,600 visibility data points. In this case, The SNR of the reconstructed image using the multi-feature algorithm is 23.8 dB, which is slightly higher than that using 504,720 visibility data points.

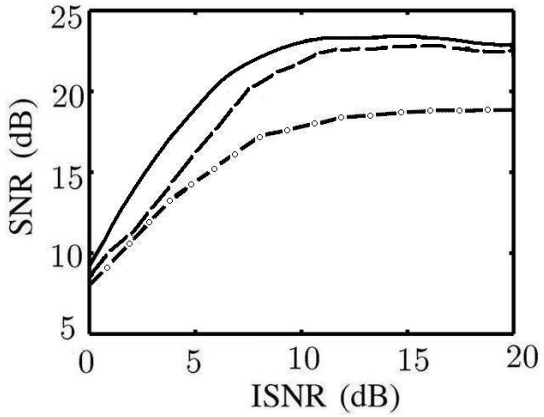

Fig. 3. Average SNR as a function of ISNR, over 100 realizations, ——: multi-feature algorithm on 15,141,600 visibility data, ------: multi-feature algorithm on 504,720 visibility data, --o--:: MS-CLEAN algorithm [9] on 504,720 visibility data.

IV. Conclusion

A multi-feature algorithm is proposed to reconstruct the visibility distribution instead of the image itself. The visibility data are categorized into four different feature regions, depending on the configuration of stations and the object to be observed. Up to 15,000,000 visibility data points have been processed in the simulations, based on the LOFAR configuration. Compared with the conventional algorithms like PURIFY and MS-CLEAN algorithms, the computational time can be reduced by a few hundreds to one thousand times, and expected to be even more if the amount of data is increased.

References

[1] J. W. M. Baars, L. R. D'Addario, and A. R. Thompson, "Radio astronomy in the early twenty-first century," Proc. IEEE, vol.97, no.8, pp.1377-1381, Aug. 2009.

[2] U. Rau, S. Bhatnagar, M. A. Voronkov, and T. J. Cornwell, "Advances in calibration and imaging techniques in radio interferometry," *Proc. IEEE*, vol.97, no.8, pp.1472-1481, Aug. 2009.

[3] S. Johnston, M. Bailes, N. Bartel, C. Baugh *et al.*, "Science with the Astralian square kilometre array pathfinder," *Pub. Astronom. Soc. Australia*, vol.24, pp.174-188, Dec. 2007.

[4] S. J. Tingay, R. Goeke, J. D. Bowman *et al.* "The Murchison widefield array: The square kilometre array precursor at low radio frequencies," *Pub. Astronom. Soc. Australia*, vol.30, e007, 2013.

[5] J. L. Jonas, "MeerKAT - The South African array with composite dishes and wide-band single pixel feeds," *Proc. IEEE*, vol.97, issue 8, pp.1522-1530, Aug. 2009.

[6] P. E. Dewdney, P. J. Hall, R. T. Schilizzi, and T. J. L. W. Lazio, "The square kilometre array," *Proc. IEEE*, vol.97, issue 8, pp.1482-1496, Aug. 2009.

[7] D. V. Marco, W. G. Andre, and N. Ronald, "The LOFAR telescope: System architecture and signal processing," *Proc. IEEE*, vol.97, no.8, pp.1431-1437, Aug. 2009.

[8] I. Griva, G. N. Stephen, and S. Ariela, *Linear and Nonlinear Optimization*, Soc. Indust. Applied Math., ch.13, 2009.

[9] T. J. Cornwell, "Multiscale CLEAN deconvolution of radio synthesis images," *IEEE J. Select. Topics Signal Process*., vol.2, no.5, pp.793-801, Oct. 2008.